MACKPESQUISA

RELATÓRIO FINAL

PROJETO:

Desenvolvimento de Fontes Ópticas à Taxa de 40 GHz e Aplicações em Redes com Densa Multiplexação por Divisão do Comprimento de Onda (DWDM) – PARTE II

por
Eunézio A. de Souza

Índice:

Campus São Paulo: *Rua da Consolação, 896 ● Consolação ● São Paulo - SP ● CEP 01302-907*
Tel. (11) 3236-8444/8633 ● www.mackenzie.br/mackpesquisa
mackpesquisa@mackenzie.br

RELATÓRIO FINAL DO PROJETO DE PESQUISA

PROJETO DE PESQUISA: DADOS
Solicitante: **Eunézio Antônio de Souza**
Título do Projeto: ***Desenvolvimento de Fontes Ópticas à Taxa de 40 GHz e Aplicações em Redes com Densa Multiplexação por Divisão do Comprimento de Onda (DWDM) – Parte II***
Unidade: **Centro de Ciências e Humanidades**
Área de Conhecimento: **Sistemas de Telecomunicações**
Linha de Pesquisa: **Sistemas de Comunicações Ópticas e Fotônica**

1. PROJETO DE PESQUISA

Os objetivos do projeto (com duração prevista de 3 anos) divididos em três etapas, das quais duas foram severamente prejudicadas pela quebra de componentes e pelo atraso na impostação. Entretanto, utilizando os equipamentos disponíveis no laboratório, demos andamento a atividades correlatas a este projeto e os seus resultados foram apresentados nas melhores conferências da área, tais como:

- Conference on Laser and Eletrooptics (CLEO-2010),
- Frontiers of Optics (FIO-2010),
- Laser and Eletrooptic Society (LEOS-2009),
- International Microwave Conference (IMOC-2009 e 2010),
- X - Encuentro Latinoamericano de Óptica, Láseres y sus Aplicaciones (Optilas-2010),
- Ultrafast Phenomena (UP-2010) e
- Latin America Optics and Photonics Conference (LAOP-2010).

Na primeira etapa (*Construção de um laser de femtossegundos de fibra dopada com Érbio operando a taxa de 40 GHz*) tivemos problemas, e ainda estamos tendo, com importação de equipamentos com defeito. Foram comprados dois moduladores, um de amplitude e outro de fase, e ambos apresentaram problemas. Estes problemas foram parcialmente solucionados no final de 2010, pelo setor de importação do Mackenzie, e esperamos em breve obter os primeiros resultados.

Na segunda etapa (*Construção uma fonte baseada no batimento de freqüência entre dois lasers*), apresentamos (no relatório anterior) um estudo sobre fontes de altas taxas baseadas em efeitos não-lineares. Primeiramente foram descritas as principais características das fibras ópticas, assim como a propagação da luz nas mesmas, em seguida são demonstrados seus efeitos lineares e não-lineares. Este estudo foi também comprometido pela falta do autocorrelador. A situação já está normalizada e esperamos em breve obter melhores resultados.

Na terceira etapa (*Simulação do desempenho da transmissão de sistemas WDM a 40 GHz*) investigamos um link de transmissão DWDM de 40 Gbit/s RZ DQPSK, sem repetição, usando apenas amplificadores de fibra dopada com Érbio (EDFAs). Demonstramos também a transmissão por mais de 1800 km de 10 canais DWDM a 40 Gb/s RZ-DQPSK com 50 GHz de espaçamento empregando uma PCF para compensar a dispersão residual.

Campus São Paulo: *Rua da Consolação, 896 ● Consolação ● São Paulo - SP ● CEP 01302-907*
Tel. (11) 3236-8444/8633 ● www.mackenzie.br/mackpesquisa
mackpesquisa@mackenzie.br

2. DESCRIÇÃO DAS ETAPAS EXECUTADAS:

2.1. SBS impairments at 40 Gb/s RZ DQPSK DWDM unrepeatered transmission

Suzanne Susskind, Fulvio Ceragioli and Eunézio Antônio de Souza
Universidade Presbiteriana Mackenzie, Laboratório de Fotônica
Rua da Consolação 896, São Paulo, 01213-907, Brazil

Abstract. We investigate an unrepeatered DWDM transmission link at 40 Gb/s using RZ DQPSK with only Erbium-doped fiber amplifiers (EDFAs). No in-line or pre dispersion compensation was used in the system. The channels were distributed ranging from 1561 nm to 1563.8 nm, with 50 GHz of channel spacing. We only post compensate the dispersion by a dispersion compensated fiber (DCF). The nonlinearities impairments for a four and eight channel transmission were evaluated, and we find significant SBS suppression comparing four and eight channel transmission.

1. Introduction

Over the years, technology advances have significantly increased the system capacity and reach for 10 Gb/s and 40 Gb/s unrepeatered transmissions. This systems aim to provide high capacity over long distances without any in-line active elements, consequently reduce the line complexity and the overall system cost. To achieve long single-span distances, system architects may resort to high launch powers, alternative modulation formats, very low-loss fibers, a high-power booster, distributed Raman amplification, etc.

However, it is desirable to simplify systems as much as possible to minimize cost, and this aim can be furthered by using fiber with lower attenuation [8] and launching channel powers as high as possible. However, the limiting factor for high launch power level is often Stimulated Brillouin Scattering (SBS), a single channel optical nonlinear impairment. SBS plays an increasing role at higher power levels and can limit the performance of such networks and degrade the signal quality. On the other hand, it has been shown that system performance can be improved via SBS suppression by taking advantage of the phase modulation induced by cross-phase modulation (XPM) in wavelength-division multiplexing (WDM) systems [9,10].

Recent results was shown, like SBS mitigation and transmission improvement from cross-phase modulation at 10 Gb/s [7], eight 40 Gb/s RZ-DQPSK channels transmission over 401 km, with no in-line dispersion compensation or pre-dispersion compensation [1], ultra-long-span 500 km 16x10 Gbit/s WDM unrepeatered transmission was demonstrated with Raman amplification in combination with enlarged effective area SMF and conventional SMF [2] and also 485 km unrepeatered 4x43 Gb/s WDM NRZ-DPSK transmission with remote optically pumped amplifier (ROPA) [3].

In this work, we investigate a DWDM unrepeatered transmission at 40 Gb/s using RZ DQPSK format. The DQPSK signal has often been used with RZ pulse carving because the RZ format has better sensitivity than the nonreturn-to-zero (NRZ) format and enlarges the tolerance to optical fiber nonlinearity [4,5]. We explore further the system performance improvements obtainable from XPM effects in unrepeatered DWDM systems at 40 Gb/s and 50 GHz of channel spacing.

A simple long unrepeatered systems amplified with only erbium-doped fiber amplifiers (EDFAs) was used. No in-line or pre dispersion compensation was used in the system. We only post compensate the dispersion by a dispersion compensated fiber (DCF).

We compare system performance for DWDM transmission with different channel counts as a function of transmission distance and post dispersion compensation values. The nonlinearities impairments were also shown and we find significant Stimulated Brillouin Scattering (SBS) suppression in DWDM systems for different numbers of channels.

2. System configuration

The simulation model is depicted in Figure 1. The transmitter consists of a DFB laser diode with 50 GHz channel spacing. The channels are modulated at 40 Gb/s RZ DQPSK format with a Mach-Zehnder (MZM) external modulator with a sequence length of 2^{23}-1.

We investigate the transmission of a single, eight and sixteen DWDM channels, which were distributed ranging from 1557.8 nm to 1563.8 nm, with 50 GHz of channel spacing.

The signal was amplified by a high power EDFA booster amplifier with output power controlled. The DWDM signal was launched into the unrepeatered transmission link, which consists of 160 km of SSMF, represented by the Kyatera Network distance between São Paulo and Campinas (Brazil). KyaTera Network has 33 institutions interconnected through a fiber-to-the-lab optical network dedicated to research working remotely from their institutions in a cooperative way.

The average loss of the transmission fiber in the link was 0.2 dB/km, and the dispersion at 1560 nm was 17.5 ps/nm.km. The effective area was about 80 μm^2 and the nonlinear index was $2.6e^{-20}$ m^2/W.

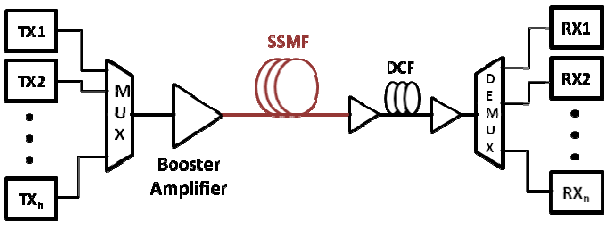

Figure 1. Model scheme of the transmission system simulated.

A second EDFA was used to compensate the attenuation and the output power is controlled to guarantee a low input power at the DCF and then the system would not be limited by nonlinearities. Only post dispersion compensation was used in the system by a DCF. The DCF employed has approximately -250 ps/nm.km of dispersion, 0.5 dB/km of attenuation and 15 μm^2 of effective area. A preamplifier is employed to maintain good receiver responsivity.

After transmission, a 40 GHz bandwidth filter was used to select the DWDM channel. At the RZ DQPSK receiver the signal decoding is optical performed by MZ interferometers and detected by PIN photodiode, with a responsivity of 0.8 A/W. Then a clock and data recovery was employed followed by a low pass post detection filter. The recovered data signal was passed to a bit error rate tester (BER) for measurement of the signal BER. A simple Forward Error Corrector (FEC) was also employed.

3. Simulation results

With the propose of evaluate the transmission distance in function of total system dispersion, we initially examine the maximum SMF length regarding the DCF length. The transmission output power was fixed in 9 dBm/channel, and we consider a BER value equal to $1e^{-9}$. Figure 2 shows the SMF length in function of DCF length, for 1, 8 and 16 channels transmission. We could see that the SMF length increases linearly for the 3 transmission cases; therefore as the DCF length increases, the length of the transmission fiber grows linearly. We also could notice that for all SMF length, the optimum DCF length founded which guarantees a BER of $1e^{-9}$ provides a total system dispersion of about 300 ps/nm. Above 250 km of SMF the booster output power should be increased to supply attenuation effects.

The system performance versus channel launch power for a single, 8 and 16 channel transmission was evaluate, as shown in Figure 3 (a). The BER was analyzed for DWDM systems and single channel transmission for the same 1561 nm channel. For this analysis, the SMF length was fixed in 160 km, corresponding to the Kyatera Network length, the DCF length in 12 km and the output power of the second EDFA was set in 10 dBm/channel.

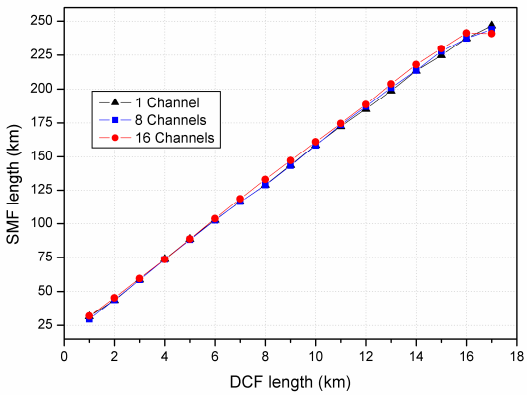

Figure 2. SMF length in function of DCF length for a BER equal to $1e^{-9}$.

Campus São Paulo: *Rua da Consolação, 896 ● Consolação ● São Paulo - SP ● CEP 01302-907*
Tel. (11) 3236-8444/8633 ● www.mackenzie.br/mackpesquisa
mackpesquisa@mackenzie.br

As observed in Figure 3 (a), the BER decrease for 8 and 16 channel transmission, compared to single channel transmission, mainly at high input power. This result presents the SBS influence and limitation in single channel system performance. As the channel power increases in the DWDM systems featuring the beginning of XPM effect, the systems significantly suppresses the SBS impairment and improves the signal quality [7].

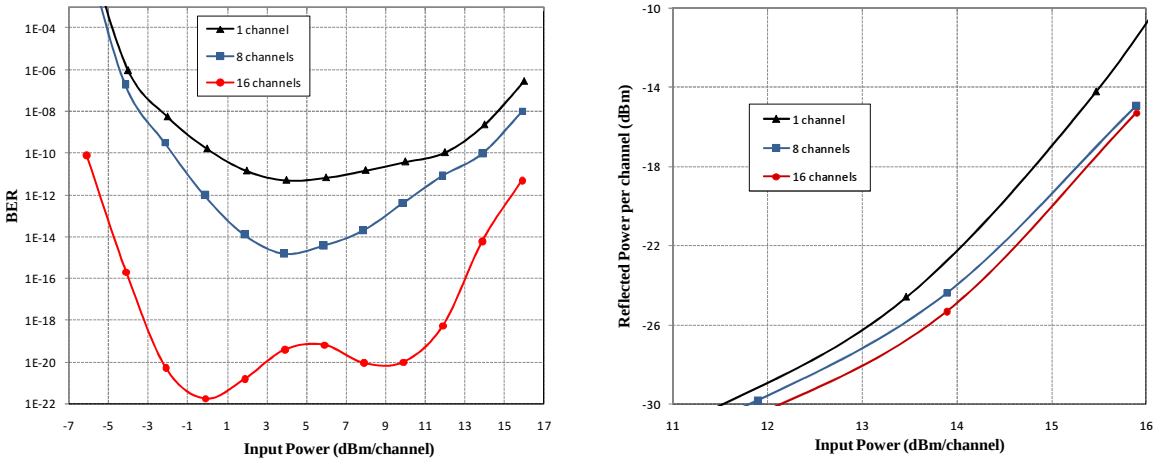

(a) (b)

Figure 3. (a) BER values versus channel launch power for a single, 8 and 16 channel transmission (b) Reflected power per channel (dBm) against input power per channel (dBm).

To verify that the improved signal quality obtained in the DWDM system was due to SBS suppression by XPM effect, we measured the reflected power of the three transmission cases. The results are shown in Fig. 3 (b), in which the reflected power per channel is plotted against the launch power per channel. The launch power levels of the DWDM channels were all the same.

We could see a reduction of reflected power in the DWDM system configurations assigned to SBS effect. As channel power is increased induce phase modulation effects that can significantly reduce the SBS impairment in comparison to the single channel case [6]. For that reason, the system performance for 16 channel transmission, showed in Figure 3 (a), are much better than single channel transmission.

To quantify the SBS impairments, we broaden the laser linewidth from 0 to 350 MHz and evaluate the system range, represented by SMF length for a single channel transmission. The input power and total accumulated dispersion of the system was also analyzed. These results are shown in Figure 4, and we take into account a BER value of $1e^{-9}$.

As shown in Figure 4, for negative total accumulated dispersion, as the laser linewidth brodens, the channel reaches more long distances, mainly for high input power. As a result, the SBS effect is reduced. For positive total accumulated dispersion the opposite occurs, as we narrow the laser linewidth the signal achieves longer distances. For long distances, the signal espectral broden by fiber dispersion, therefore narrow the laser linewidth is good for better performance.

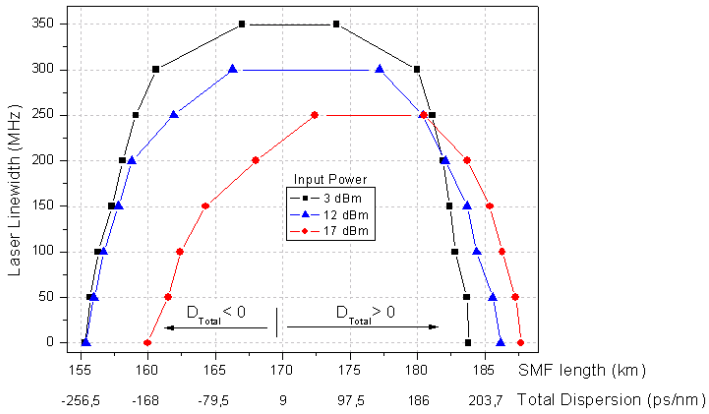

Figure 4. Laser linewidth (MHz) versus SMF length (km) and total dispersion (ps/nm) for a single channel transmission, considering an input power of 3, 12 and 17 dBm.

Campus São Paulo: *Rua da Consolação, 896 ● Consolação ● São Paulo - SP ● CEP 01302-907*
Tel. (11) 3236-8444/8633 ● www.mackenzie.br/mackpesquisa
mackpesquisa@mackenzie.br

Figure 5 shows the BER values over the transmission fiber, using 12 km of DCF to compensate the system dispersion. We analyzed the transmission of a single channel, 8 and 16 channels. In all cases, the last channel limits the transmission, mainly because it is the channel with the higher accumulated dispersion.

For eight channel transmission the SMF length reached 184 km and for sixteen channel transmission, achieved about 185 km, considering in both cases a BER value of $1e^{-9}$. The sixteen channels DWDM system presented better performance compared with a eight channel transmission. The accumulated dispersion was about 275 ps/nm for eight channels transmission and 290 ps/nm for sixteen channels.

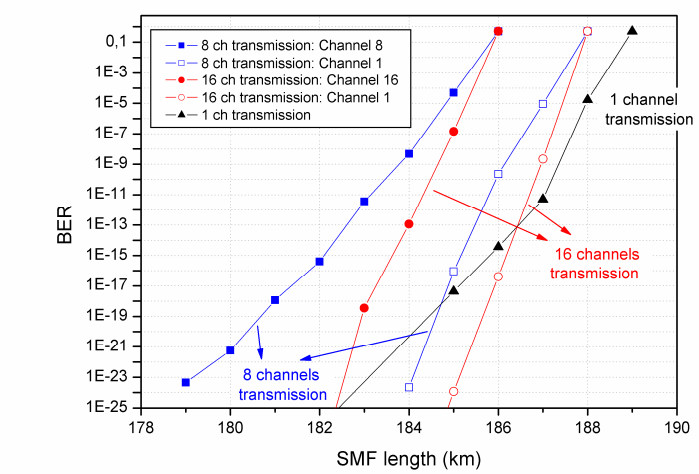

Figure 5. BER as a function of transmission fiber length (SMF) with 12 km of DCF for a single, 8 and 16 channel transmission.

4. Conclusions

In this work, we investigate simple long unrepeatered systems at 40 Gb/s using RZ DQPSK signals and 50 GHz of channel spacing. We only post compensate the dispersion by a dispersion compensated fiber and the signal is amplified only by EDFAs.

We present the SBS influence and limitation in a single channel system performance, comparing with DWDM systems. We show that the DWDM systems significantly suppress the SBS impairment and improve the signal quality, by the beginning of XPM effect.

The SBS effect is reduced for negative total accumulated dispersion, the channel reaches more long distances at high input power, as the laser linewidth brodens. For positive total accumulated dispersion the opposite occurs.

We also compare system performance for DWDM transmission as a function of transmission distance. Using 12 km of DCF, the 8 channels DWDM signal could reach 184 km and for 16 channels, 185 km, with a good performance limited by the last channel.

References

[1] J.-X. Cai, B. Bakhshi, and M. Nissov, “Transmission of 8x40 Gb/s RZ-DQPSK Signals Over a 401 km Unrepeatered Link”, OFC/NFOEC 2008, OMQ5.

[2] H. Maeda, G. Funatsu and A. Naka, “Ultra-long-span 500km 16x10 Gbit/s WDM unrepeatered transmission using RZ-DPSK format”, Electron. Lett. 41, pp. 34-35, 2005.

[3] P. Bousselet, D. A. Mongardien, P. Brindel, H. Bissessur, E. Ditusseuil, E. Brandon, I. Brylski, “485 km unrepeatered 4x43 Gb/s NRZ-DPSK transmission”, OFC/NFOEC 2008, OMQ7.

[4] C. Xu, X. Liu, L. Mollenauer, and X. Wei, “Comparison of return-tozero phase shift keying and on-off keying in long haul dispersion managed transmissions”, in Proceedings OFC 2003, Atlanta, GA, Mar. 2003, Paper ThE3, pp. 453–454.

[5] N. Yoshikane and I. Morita, “1.14 b/s/Hz Spectrally Efficient 50 85.4-Gb/s Transmission Over 300 km Using Copolarized RZ-DQPSK Signals”, Journal of Lightwave Technology, vol. 23, nº. 1, January 2005, pp. 108-114.

Campus São Paulo: *Rua da Consolação, 896 ● Consolação ● São Paulo - SP ● CEP 01302-907*
Tel. (11) 3236-8444/8633 ● www.mackenzie.br/mackpesquisa
mackpesquisa@mackenzie.br

[6] Y. Horiuchi, S. Yamamoto, and S. Akiba, "Stimulated Brillouin scattering suppression effects induced by cross-phase modulation in high power WDM repeaterless transmission," IEE Electronics Letters vol. 34, 1998, pp. 390-391.
[7] J. D. Downie and J. Hurley, "Experimental study of SBS mitigation and transmission improvement from cross-phase modulation in 10.7 Gb/s unrepeatered systems", Optics Express, vol. 15, nº 15, 23 July 2007, pp. 9527-9534.
[8] J. D. Downie, J. Hurley, R. Khrapko, D. Ma and S. Gray, "Performance comparison of a new low attenuation fibre with G.652 fibre in unrepeatered single-span systems," Proceedings ECOC 2006, Cannes, France, September 2006, Paper Mo3.3.3, pp. 1-2.
[9] Y. Horiuchi, S. Yamamoto, and S. Akiba, "Stimulated Brillouin scattering suppression effects induced by cross-phase modulation in high power WDM repeaterless transmission," IEE Electron. Lett. 1998, vol. 34, pp. 390-391.
[10] S. S. Lee, H. J. Lee, W. Seo, and S. G. Lee, "Stimulated Brillouin scattering suppression using cross-phase modulation induced by an optical supervisory channel in WDM links," IEEE Photon. Technol. Lett. 2001, vol. 13, pp. 741-743.
[11] J. M. C. Boggio, J. D. Marconi, and H. L. Fragnito, "Experimental and numerical investigation of the SBS-threshold increase in an optical fiber by applying strain distributions," J. Lightwave Technol. 2005, vol. 23, pp. 3808–3814.

2.2. DWDM 40 Gb/s Long Haul Transmission using PCF for dispersion compensation

Suzanne Susskind[(1)], Marcos A. R. Franco[(2,3)], Valdir A. Serrão[(2)] and Eunézio A. de Souza[(1)].
[(1)] *Universidade Presbiteriana Mackenzie, Laboratório de Fotônica, Rua da Consolação 896, São Paulo, 01213-907, Brazil*
[(2)] *Instituto de Estudos Avançados (IEAv), Rod. dos Tamoios, km 5.5, São José dos Campos-SP, 12228-001, Brazil*
[(3)] *Instituto Tecnológico de Aeronáutica – ITA, Pr. Marechal Eduardo Gomes, 50, São José dos Campos-SP, 12228-900, Brazil*
suzanne.susskind@osamember.org

Abstract: We demonstrate a 10 channels DWDM transmission at 40 Gb/s RZ-DQPSK with 50 GHz of channel spacing over 1800 km employing a multicore PCF to compensate the link residual dispersion instead of dispersion compensating fibers.

1 - Introduction

Transmission at 40 Gb/s and higher is severely affected by dispersion slope penalty. This effect that highly limits the transmission should be compensated, so dispersion compensation is indispensable for long distance high speed transmission. To obtain large negative dispersion coefficient, such as DCF, usually a highly Ge-doped central core is required leading to higher losses and fabrication difficulties. To overcome these problems, PCF has been proposed, mainly because of the efficiency for chromatic dispersion management and the possibility to obtain even −10000 ps/(nm·km) dispersion coefficient without Ge doping [1].

Recently, employing transmission of 10 channels DWDM RZ DQPSK at 40 Gb/s has been demonstrated over 1000 km using DCFs to dispersion compensation [2]. Here, we successfully transmitted 10 channels DWDM at 40 Gb/s RZ DQPSK over 1800 km, and we used only PCFs to compensate the dispersion.

2 - System Configuration

The scheme of the simulation model is shown in Fig. 1. The transmitter consists of a DFB laser diode with wavelengths ranging from 1560.20 nm to 1563.86 nm with 50 GHz channel spacing. The channels were modulated at 40 Gb/s RZ DQPSK format with a Mach-Zehnder (MZM) external modulator with a sequence length of 2^{23}-1.

The signal was transmitted through the system which consists of N spans of a SMF immediately followed by a dispersion compensated photonic crystal fiber (DCPCF). Each span was post dispersion compensated to reduce the nonlinear effects induced by high span input power. Optimized structural parameters for DCPCF are Λ = 1.5356 μm, d/Λ = 0.3444 and d_r/Λ = 0.2733 where d is the hole diameter, Λ is the hole pitch of triangular lattice structure and the outer ring core is formed by reducing the diameter of air holes in i-th ring to d_r, presented by T. Fujisawa et al. [1]. The average dispersion is -174 ps/nm.km and the effective area is 23.3 μm^2. The spans fibers lengths of SMF and DCPCF were fixed in 80 km and 6 km, respectively.

Between the spans, EDFAs supplies a 23 dB gain to compensate spans losses. After transmission, a 40 GHz bandwidth filter was used to select a WDM channel. At the RZ DQPSK receiver the signal decoding is optical performed by MZ interferometers and detected by PIN photodiode with a responsivity of 0.8 A/W and followed by a low pass post detection filter.

The RDCF was located before the booster amplifier to pre compensates the dispersion before the link transmission. The RDCF design includes a central defected-core and six surrounding extra-cores. The multicore fiber adds extra geometric controllability for tailoring ultra-flattened chromatic dispersion. High negative dispersion could be reached allowing a large reduction of dispersion compensating fiber length. Negative dispersion of about −182.25 ps/nm.km and absolute dispersion variation of ΔD ~2.3 ps/nm/km could be reached over E + S + C + L + U wavelength bands. The main geometric parameters of RDCF design, presented in [3] are the distance of consecutive air-holes (Λ=2.0 μm) and the air-hole diameters (d =1.4 μm) at cladding region, the distance of consecutive air-holes (Λ_c=0.488 μm) and the air-hole diameters (d_c=0.35 μm) at central defected-core and the air-hole diameters (d_m= 1.117 μm) at extra-cores. Fig. 2 presents the ultra-flattened negative dispersion obtained for RDCF with six extra cores. The average dispersion is −178.55 ps/nm.km with absolute dispersion variation of ΔD ~ 0.017 ps/nm/km over band C.

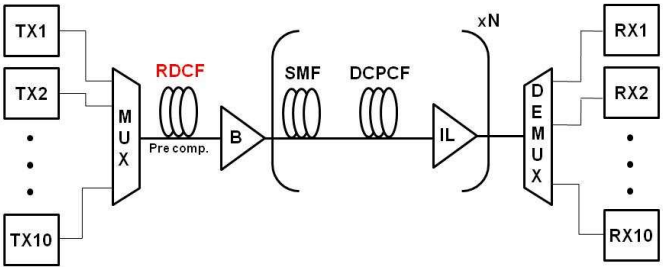

Fig 1. Model scheme of the transmission system simulated.

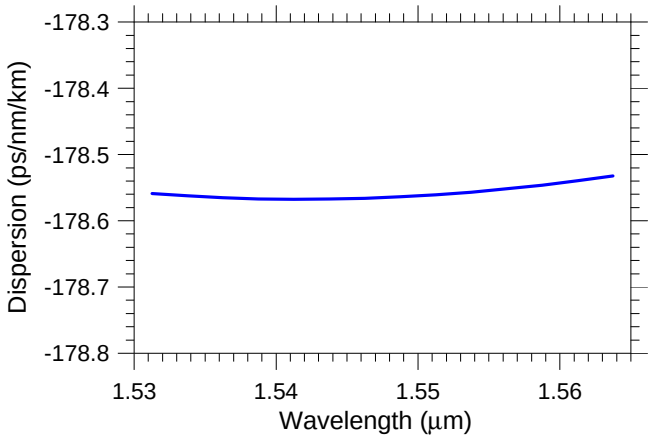

Fig 2. Ultra-flattened negative dispersion of RDFF over all band C.

3 - Results

The transmission without RDCF pre compensation reached 1200 km limited by channel 10, which has the largest amount of residual dispersion. Then, the dispersion pre compensation is adjusted for best BER performance. With the inclusion of 39 km and 40 km of RDCF the transmission increased to 1700 km and 1800 km, respectively, with a BER of $1e^{-9}$, as shown in Fig. 3.

Campus São Paulo: *Rua da Consolação, 896 ● Consolação ● São Paulo - SP ● CEP 01302-907*
Tel. (11) 3236-8444/8633 ● www.mackenzie.br/mackpesquisa
mackpesquisa@mackenzie.br

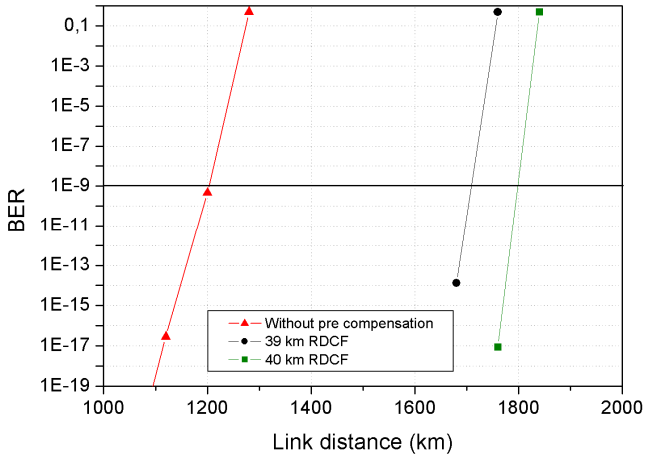

Fig 3. BER versus transmission distance for channel 10.

The residual dispersion per span is about +344 ps/nm, therefore for 1800 km of SMF the total accumulated dispersion is nearly 1174 ps/nm. The system performance would not be dependent only on the total accumulated dispersion value, but the interaction with SPM [4] and for good system performance the accumulated dispersion value must be positive. This is due to the pulse compression effect induced by SPM during propagation in the anomalous-dispersion regime [5].

The system performance with dispersion compensation by using PCF showed better results compared to the system with DCF, which reached 1000 km, showed by [2].

4 - Conclusion

We demonstrate a 10 channels DWDM transmission at 40 Gb/s RZ DQPSK and 50 GHz of channel spacing over 1800 km of SMF, without Raman amplification or special polarization multiplex. We successfully employ a 40 km of multicore photonic crystal fiber to compensate the link residual dispersion instead of dispersion compensating fibers. The RDCF used presents ultra-flattened negative dispersion, with an average dispersion of –178.55 ps/nm.km and absolute dispersion variation of $\Delta D \sim 0.017$ ps/nm/km over band C.

The choice for PCF, which presents unique propagation properties as single mode operation over large wavelength range, high birefringence, high or low non-linearity and tailored chromatic dispersion profile, demonstrated such special properties that have stimulated innovative designs and applications for optical communications.

Acknowledgment

This work was supported by INCT FOTONICOM and Fundo Mackenzie de Pesquisa (MACKPESQUISA).

References

[1] T. Fujisawa, K. Saitoh, K. Wada, and M. Koshiba, *"Chromatic dispersion profile optimization of dual-concentric photonic crystal fibers for broadband dispersion compensation"* Opt. Express, vol. 14, no. 2, 2006, pp. 893–900

[2] Suzanne Susskind and E.A. de Souza, *"40 Gb/s RZ DQPSK transmission with SPM and ASE suppression by dispersion management"*, International Microwave and Optoelectronics Conference (IMOC), 3-6 Nov. 2009, Belém, Pará, pp. 106-109

[3] Marcos A. R. Franco, Valdir A. Serrão, and Francisco Sircilli, *"Microstructured Optical Fiber for Residual Dispersion Compensation Over S+C+L+U Wavelength Bands"*, IEEE Photonics Technology Letters, V. 20, nº 9, May 1, 2008, pp 751-753

[4] A. H. Malik, M. Azeem, M. Y. Hamza, S. Tariq, *"Comparison of Interaction of GVD and SPM Between Normal and Anomalous Dispersion Regimes of Single Mode Fiber"*, Second International Conference on Electrical Engineering University of Engineering and Technology, Lahore (Pakistan), 25-26 March 2008, 6p

G. Bellotti, A. Bertaina, S.Bigo, *"Dependence of Self-Phase Modulation Impairments on Residual Dispersion in 10-Gb/s-Based Terrestrial Transmissions Using Standard Fiber"*, IEEE Photonics Technology Letters, V. 11, Nº. 7, 1999, pp. 824-826

Campus São Paulo: *Rua da Consolação, 896 ● Consolação ● São Paulo - SP ● CEP 01302-907*
Tel. (11) 3236-8444/8633 ● www.mackenzie.br/mackpesquisa
mackpesquisa@mackenzie.br

2.3. Study of SWCNT Diameter Influence on Mode-Locked Erbium-doped Fiber Laser Performance

H. G. Rosa, P. G. Komninos and E. A. de Souza
Photonics Laboratory, Mackenzie University, Rua da Consolação 896, 01302-907, São Paulo, Brazil
henriquehgr@mackenzista.com.br

Abstract: This paper presents a study about output bandwidth maximization in Erbium-doped fiber lasers, by using thin films incorporating Carbon Nanotubes (CNT) with diameters of 0.8 and 1.0 nm, with several films transmittance values and different total cavity dispersion. Best result was achieved with 1.0 nm CNT generating a maximum bandwidth of 5.7 nm when films transmittance is 37%.

OCIS codes: (140.3500) Lasers, Erbium; (140.4050) Mode-locked Lasers; (160.4236) Nanomaterials.

1. Introduction

Studies had been performed about characterization and applications of Carbon Nanotubes (CNT), due to its attractive electrical and optical properties, such as fast exciton recovery time (< 1 ps) [1], and semiconductor structure E_{gap} between 0.5 and 1.2 eV [2], which places its absorption on IR spectral range. CNT show IR saturable absorption to low light intensities, typically 2.5×10^5 W/m^2, and can be used as mode-locker to rare-earth-doped fiber lasers. For ultrashort pulses and broadband spectra generation optimization, theoretical and experimental studies point out that there is an optimal relation between laser wavelength operation and CNT diameter [3].

Carbon Nanotubes can be incorporated into laser cavities by several techniques, mainly optically-driven deposition [4] on fiber end, and polymer thin films incorporating carbon nanotubes [5]. In this work we adopted the polymer films incorporating CNT method, due to its reliability and simple control on films thickness, concentration and absorption. This paper reports the fabrication and use of CNT thin films for application as saturable absorber mode-locker in Erbium-doped fiber lasers. We present a study about output bandwidth optimization in Erbium-doped fiber laser, involving CNT diameter and films transmittance.

2. Experimental Design

We fabricated thin films incorporating CNT by a new and simple method developed by us [6]. In this study, we used two kinds of high purity single-walled CNT, one with a mean diameter of 0.8 nm, and the other with 1.0 nm. As host polymer, we choose NOA 73™ (a urethane-based compound used as optical adhesive), due to its high transparency (95%) to infra-red light and its refraction index (1.56) close to silica index. The CNT films were than matched between APC ferrules of optical fibers to form all-optical saturable absorber samples, as shown in figure 1a and 1b. As a main parameter to classify the samples, we adopted the non-saturated αL product [7], related to sample absorption strength.

By this method, we were able to set up several samples with different features. First, we have three different CNT films concentrations: 1, 2 and 4 mg/ml. With the 1 mg/ml CNT film, we were able to make samples with αL values varying between 0.18 and 0.38, corresponding to high transmittance values. With the 2 and 4 mg/ml films, we fabricated samples with αL values varying between 0.4 and 1.5, covering values of films transmittance coming from 20% up to 70 %.

Fig. 1. a) Thin film incorporating CNT at the fiber connector end; b) sample containing CNT film; c) Mode locked EDFL set up.

To test our saturable absorbers CNT samples, we built an Erbium-doped fiber laser, ring cavity, as shown in figure 1c. Our laser is 1480 nm pumped, P_{pump}(max) = 340 mW, and has a emission peak at 1559 nm, $P_{24\%\ output}$ (max) = 3.5 mW. In the simplest configuration, the total cavity length is 5 m, and the cavity dispersion is -0.108 ps^2.

3. Results

By using our saturable absorber samples, we were able to obtain self-start mode-locking. Due to the random orientation of CNT in our films, mode-locking is practically independent on polarization state. However polarization plays an important role on laser optimization. It is possible to find a polarization state of light that maximizes the laser output bandwidth, allowing to achieve shorter pulses.

Laser output bandwidth is also quite sensitive to CNT diameter. We performed a study about laser output spectrum as a function of CNT diameter and αL product of saturable absorber samples. We focused our results on maximum bandwidth generation, for future applications in spectrally sliced WDM systems as broadband laser sources. We changed the laser cavity dispersion by changing the length of SSMF inside cavity. Results of the mode-locked Erbium-doped fiber laser achieved by using 0.8 nm diameter CNT are shown in figure 2a, and results by using 1.0 nm diameter CNT in figure 2b.

a) b)

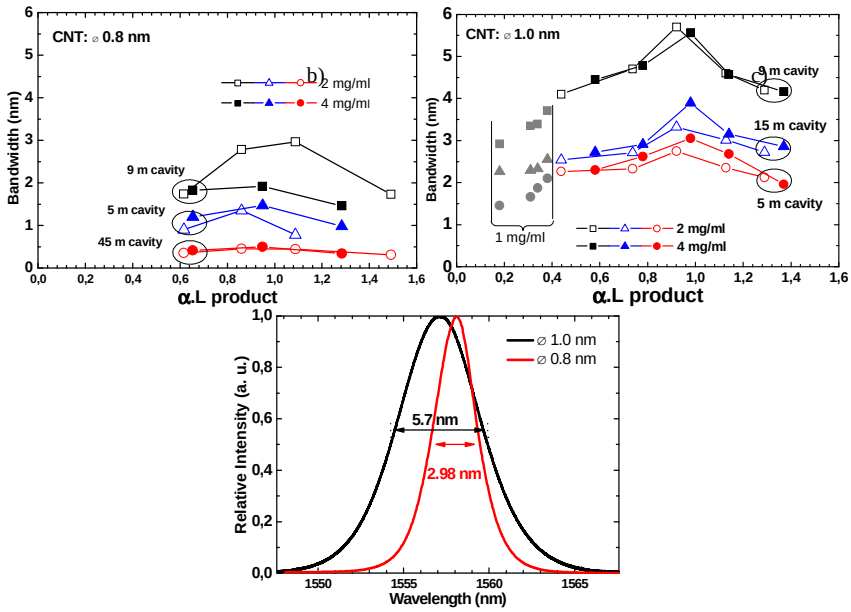

Fig. 2. Output spectrum bandwidth as a function of αL product of saturable absorber samples with CNT mean diameter of a) 0.8 nm, and b) 1.0 nm. We verified the largest output bandwidth for each αL value for many laser cavity dispersion: 5 m, -0.108 ps^2; 9 m, -0.195 ps^2; 15 m, -0,324 ps^2; 45 m, -0,973 ps^2; c) comparison between largest bandwidth for both CNT diameters.

As shown in fig 2, we experimentally confirmed that 1.0 nm diameter CNT is more suitable for operation at 1550 nm. The bandwidth generated with those ones was at least 91% larger than bandwidth generated with 0.8 nm diameter CNT, as shown in figure 2c. We also could identify that saturable absorber samples seems to be independent on films concentration, and bandwidth depends only on saturable absorber αL product and cavity dispersion. Other important results is that there are optimal values for bandwidth optimization: the optimal αL product value to a laser like used in this work is approximately 1.0, i. e., maximum bandwidth is generated when samples transmittance is close to 37%; and also for maximum bandwidth generation there is an optimal cavity dispersion value, of -0.195 ps², corresponding approximately to a 9 m long cavity. Reducing cavity dispersion close to zero dispersion value does not lead to higher bandwidths. As cavity dispersion is decreased, gain filtering effect [8] plays a role on bandwidth shortening, preventing shorter pulses and broadband spectra formation.

4. Conclusion

We fabricated thin films incorporating CNT to mode-lock Erbium-doped fiber lasers, using CNT with 0.8 and 1.0 nm diameters, and obtaining saturable absorber samples with αL values between 0.18 and 1.5. In the mode-locked laser, we obtained larger bandwidth with 1.0 nm CNT, demonstrating that 1.0 nm CNT is more suitable to 1550 nm wavelength than 0.8 nm CNT. A maximum bandwidth of 5.7 nm was obtained to CNT saturable absorber sample transmittance close to 37% (αL = 1.0) and total cavity dispersion about -0.20 ps².

5. References

[1] Y. –C. Chen *et al*., Appl. Phys. Lett., **81**, 975 (2002).
[2] H. Kataura *et al*., Synth. Met., **103**, 2555 (1999).
[3] H. Ajiki *et al*., Phys. Rev. B, **80**, 115437 (2009)
[4] J. W. Nicholson *et al*., Opt. Express, **15**, 9176 (2007).
[5] N. Nishizawa *et al*., Opt. Express, **16**, 9429 (2008).

Campus São Paulo: *Rua da Consolação, 896 ● Consolação ● São Paulo - SP ● CEP 01302-907*
Tel. (11) 3236-8444/8633 ● www.mackenzie.br/mackpesquisa
mackpesquisa@mackenzie.br

[6] H. G. Rosa and E. A. de Souza, In IEEE LEOS Annual Meeting Conference Proceedings (IEEE, Belek-Antalya, Turkey, 2009), **pp. 687-688**.
[7] E. Hecht, *Optics* (Addison Wesley, 1990), Chap. 4.
[8] K. Kieu and F. W. Wise, In The Conference on Lasers and Electro-Optics (CLEO)/The International Quantum Electronics Conference (IQEC) (Optical Society of America, Washington, DC, 2009), **CML3**.

2.4. In-Field and in-Laboratory 50 km Ultralong Erbium Fiber Laser with Soliton Pulse Compression

Lúcia A. M. Saito and Eunézio A. De Souza
Laboratório de Fotônica, Universidade Presbiteriana Mackenzie
Rua da Consolação, 896 – 01302-907 – S. Paulo / SP – Brazil, E-mail: lucia.saito@osamember.org

Abstract: We demonstrated an in-field and in-laboratory 50 km ultralong Erbium fiber laser actively mode locked with repetition rate varying from 1 to 10 GHz where the output pulse widths were determined by the soliton regime.

OCIS codes: (060.5530) Pulse propagation and temporal solitons; (140.3500) Lasers, erbium; (140.3510) Lasers, fiber; (140.3560) Lasers, ring; (140.4050) Mode-locked lasers.

1. Introduction

Recent publications reports advances in a new area of laser science: the ultralong fiber lasers. Turitsyn et al. showed the ultralong fiber lasers with a cavity length from 75 to 270 km, which were experimentally demonstrated to have a quasi-lossless transmission [1, 2]. In these works, the optical transmission link and the cavity are the same medium and the gain was provided by distributed Raman amplification with bidirectional pumping. Another application of these giant lasers was shown by Zadok et al. for secure key distribution by using two Erbium doped fiber amplifiers (EDFA), 50 km of standard telecom fiber and two mirrors in each end of the link to set the peak reflectivity frequencies representing a key bit [3].

In this paper, we investigate the generation of solitons in two ultralong Erbium-doped fiber lasers that were designed to operate in actively mode-locked regime with a modulation frequency from 1 to 10 GHz. A comparison between the output pulse widths with Kuizenga and Siegman theory [4] demonstrated a soliton regime with intracavity pulse compression.

2. Experimental Setup

Fig. 1 shows the experimental setups of the ultralong Erbium fiber laser. It consists of 2 m of Erbium-doped fiber with bidirectional pump lasers of 980 nm with a total pump power of 270 mW, an optical isolator with 50 dB of isolation and insertion loss of 0.07 dB at 1550 nm, a polarization controller, an intensity modulator, an output coupler of 13% and two sets of standard single mode fiber (SMF). One of them, by using an installed optical link in the city of Sao Paulo [5] while the other one was made of two spools of 25.3 km each and a 1% monitoring coupler after the first SMF spool.

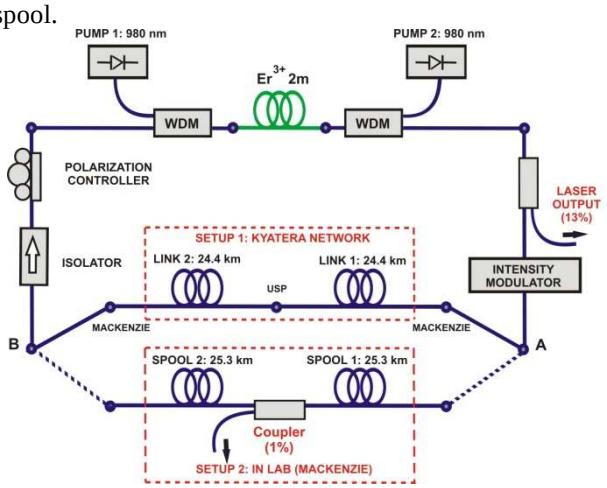

Fig. 1. Experimental setup of the two ultralong Erbium fiber lasers.

The total length of the cavity is approximately 50 km with attenuation of 13.6 dB for the in-field laser and 9.5 dB for the in-lab setup and an average intracavity dispersion of 17 ps/nm.km for both cases. For these ultralong fiber lasers, the fundamental repetition rate is about 4 kHz. Note that this spacing is very small compared to conventional lasers.

3. Results and Discussion

For the mode-locking operation, an intensity modulator was inserted into the cavity to establish repetition rate of 1, 2.5, 5, 7.5 and 10 GHz. As predicted by Kuizenga and Siegman theory [4], the pulse width produced by active mode-locking is inversely proportional to the modulation frequency as $\tau_0 \propto (1/f_m)^{1/2}$ where τ_0 is the pulse width and f_m is the modulation frequency.

Fig. 2 shows the measured output pulse width as a function of modulation frequency, with the average output power of 1.8 mW for in-field laser. For frequencies from 7.5 and 10 GHz, the duration was 67.5 and 54.8 ps respectively which were according to the theory. However, the pulse widths at the modulation frequencies of 1 GHz (97.3 ps) to 5 GHz (58.7 ps) deviate from the theoretical curve and are shorter than expected. We believe this is due to intracavity soliton compression regime.

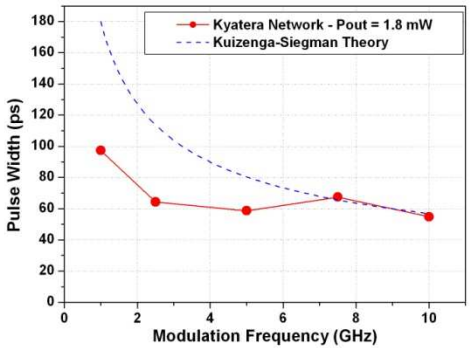

Fig. 2. Output pulse width as function of modulation frequency in active mode-locking regime for in-field laser.

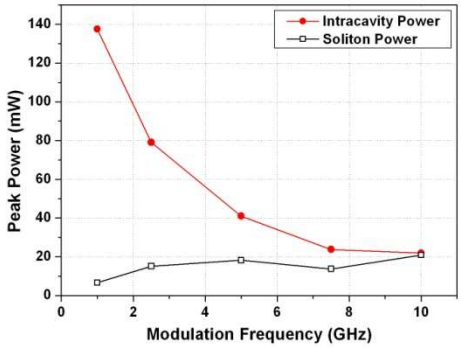

Fig. 3. Intracavity and soliton peak power versus modulation frequency for in-field laser.

Fig. 3 shows the calculated first order soliton peak power (black square curve) that is given by the expression:

$$P_0 = \frac{3.11\lambda^2|D_{ave}|}{2\pi c\gamma\,\tau_{FWHM}^2} \qquad (1)$$

where λ is the wavelength emission, D_{ave} is the average dispersion of the laser cavity, c is the velocity of light, γ is the nonlinear coefficient and τ_{FWHM} is the full width at half maximum of the pulse [6]. The values of intracavity peak power (red circle curve) were calculated considering the average output power, the pulse width showed in Fig. 2, and the respective modulation frequency in each case. Note that the intracavity peak power is higher than the soliton peak power for almost all cases and at 10 GHz we obtained N = 1 which means that below this frequency, the soliton regime is present.

We performed the same measurements in the second configuration which used two spools of 25.3 km of SMF. Fig. 4 shows the measured output pulse width as function of modulation frequency, with the same average output power of 1.8 mW.

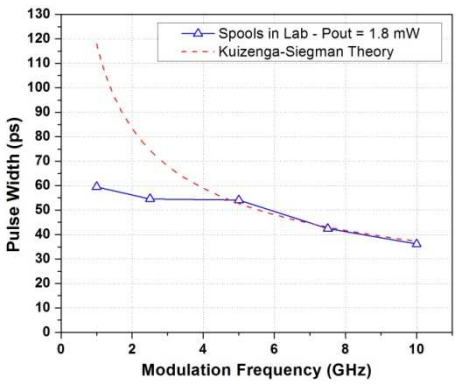

Fig. 4. Output pulse width as function of modulation frequency in active mode-locking regime for in-laboratory laser.

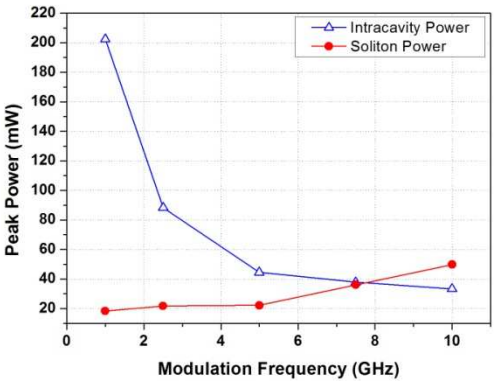

Fig. 5. Intracavity and soliton peak power versus modulation frequency for in-laboratory laser.

Campus São Paulo: *Rua da Consolação, 896 ● Consolação ● São Paulo - SP ● CEP 01302-907*
Tel. (11) 3236-8444/8633 ● www.mackenzie.br/mackpesquisa
mackpesquisa@mackenzie.br

For frequencies from 5 to 10 GHz, the duration was 54.1 to 36.1 ps which were according to the theory. However, the pulse widths at the modulation frequencies of 1 GHz (59.5 ps) and 2.5 GHz (54.6 ps) again, deviate from the theoretical curve and are shorter than expected.

Fig. 5 shows the calculated first order soliton peak power (red circle curve) and the intracavity peak power (blue triangle curve) for in-laboratory laser. Note that for frequencies below 7.5 GHz the intracavity peak power is higher than the soliton peak power. Considering the modulation frequency of 2.5 GHz, the intracavity pulse at this frequency has energy equivalent to a soliton of order 2 ($N = 2$). At 7.5 GHz we obtained $N = 1$ which is the soliton effect threshold. For higher frequencies there is no soliton regime.

In order to investigate the intracavity propagation, a comparison was made between output characteristics and the measurements after propagation in 25 km of SMF. Fig. 6a and 6b show the output pulse width with duration of 59.5 ps and corresponding optical spectrum with a FWHM of 0.066 nm at 1 GHz. The time-bandwidth product is 0.486. The inset in Fig. 6b shows the spectrum in log scale where the soliton shape with sidebands is observed [7].

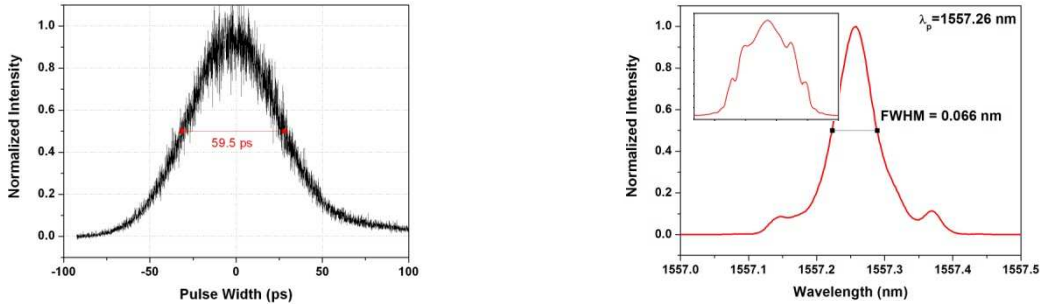

Fig. 6. (a) Output pulse width and (b) Spectrum at the modulation frequency of 1 GHz for in-laboratory laser.

Fig. 7a shows the pulse width of 41.4 ps measured in the 1% monitoring coupler after the first SMF spool at the frequency of 1 GHz. This measurement demonstrated that the pulse width is compressed along the propagation of 25 km of SMF. In addition, we can observe in the Fig. 7b the corresponding optical spectrum with FWHM of 0.075 nm. At the inset, in the log scale it is observed the soliton spectral sidebands [7]. The time-bandwidth product in this case is 0.383, close to the reference value of 0.315 for hyperbolic secant profile.

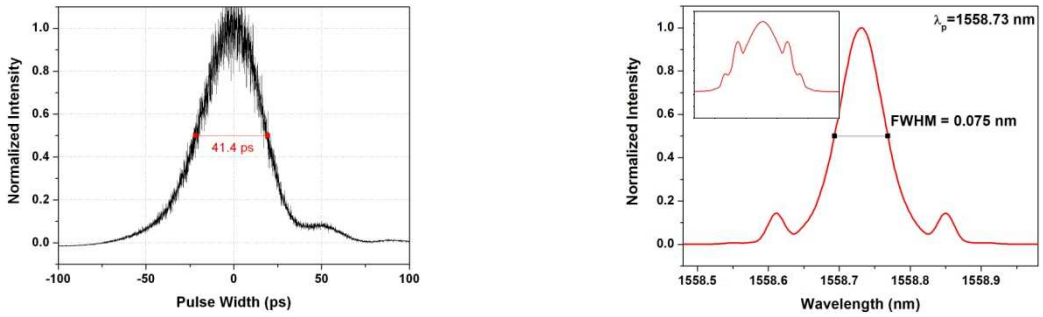

Fig. 7. (a) Pulse width and (b) Spectrum at the modulation frequency of 1 GHz after 25 km of SMF for in-laboratory laser.

4. Conclusion

In conclusion, we have demonstrated two ultralong Erbium fiber lasers, in-field and in-laboratory configurations with a cavity length of 50 km mode-locked by an intensity modulator with repetition rate varying from 1 to 10 GHz. The pulse compression occurs for high order solitons which is obtained at the modulation frequencies of 1 and 2.5 GHz for both cases. For higher frequencies, there is no soliton compression and the pulse widths are according to the standard theory of active modelocking.

5. References

[1] J. D. Ania-Castañón et al., "Ultralong Raman fiber lasers as virtually lossless optical media", Physical Review Letters **96**, 023902 (2006).
[2] S. K. Turitsyn et al., "270-km ultralong Raman fiber laser", Physical Review Letters **103**, 133901 (2009).
[3] A. Zadok et al., "Secure key generation using an ultra-long fiber laser: transient analysis and exp.", Opt. Exp. Vol. **16**, No. 21, 16680 (2008).
[4] D. J. Kuizenga and A. E. Siegman, "FM and AM mode-locking of the homogeneous laser. I – Theory", IEEE J. Quant Electron **6,** 694 (1970).
[5] Kyatera Network: www.kyatera.fapesp.br
[6] G. P. Agrawal, "Nonlinear fiber optics", Academic Press (2001)
[7] S. M. J. Kelly, "Characteristic sideband instability of periodically amplified average soliton", Electronics Letters Vol. **28**, No. 8, 806 (1992).

The authors would like to acknowledge MackPesquisa, CNPq, FAPESP and INCT FOTONICOM for financial support.

Campus São Paulo: *Rua da Consolação, 896 ● Consolação ● São Paulo - SP ● CEP 01302-907*
Tel. (11) 3236-8444/8633 ● www.mackenzie.br/mackpesquisa
mackpesquisa@mackenzie.br

2.5. Multifunctional Erbium Doped-Fiber Laser

Cláudia Barros dos Santos, E. A. de Souza
Laboratório de Fotônica - Universidade Presbiteriana Mackenzie
Rua da Consolação, 896 – São Paulo/SP – Brazil
clau.b@mackenzista.com.br

Abstract: This work present a multifunctional Erbium doped fiber laser by the use of two arrayed waveguide gratings intracavity. The experimental setup allows simultaneous operation of three regimes: passive mode-locking, continuous wave and active mode-locking.

OCIS codes: (140.0140) General; (140.3500) Lasers, Erbium; (140.3510) Lasers, Fiber.

1. Introduction

To improve data capacity transmission along communication systems, wavelength division multiplexing (WDM) sources that allows high data rates are required. Erbium-doped fiber lasers (EDFL) have always a recognized place as broad spectral width source that may be manufactured and well controlled. In this work, we present a multiplexing scheme to improve a WDM source that allows simultaneously many operating regimes of modulation at the same EDFL ring cavity.

Multiple wavelength operation of EDFL has been reported since 1992 [1] and they really can mode-locked simultaneously, but in a single repetition rate [2]. Here, we turn on three different channels in continuous wave (CW), passive mode-locked (PML), by Single Walled Carbon Nanotubes [3], and active mode-locked (AML) at 7.0 GHz regime, simultaneously, showing a potential multifunctional laser with relative simplicity at EDFL setup.

2. Experimental Setup and Results

The cavity ring laser has a laser diode pumped in 980 nm, a WDM integrating an isolator that splits pump and signal indicated by the Fig. 1a. The polarization controller (PC) was an effective way to get better performance when many channels work together. Other interesting aspect is that fact that we could analyze simultaneous regimes (fig.1b) behavior at the same output port of 16%.

A multifrequency laser (MFL) was built by integration of two arrayed waveguide gratings (AWG) within EDFL. AWGs were especially attractive due their low insertion loss, 2 to 3 dB, and low temperature sensitivity, about 0.01nm/ºC, so it is a room temperature experiment. 40 Channels accurate separated by 100 GHz and FWHM of 0.4 nm can be generated along Erbium ASE. They can be active individual or simultaneously. A great advantage is the fact that the laser has just one gain medium, about 1 meter of Erbium fiber that is capable to cover all channels providing laser emission for all of them.

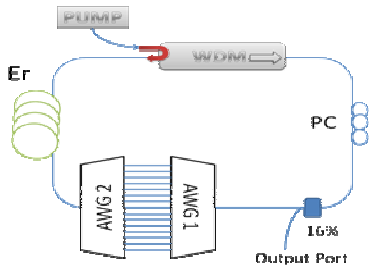

Fig. 1a) Experimental setup of EDFL including AWGs intra cavity.

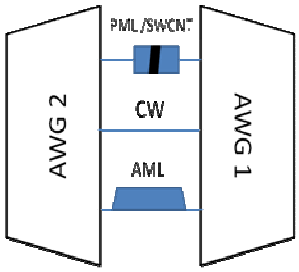

Fig. 1b) AWGs in detail when functions are turned on together.

Before insert AWGs intra-cavity, system were studied and characterized. With no AWGs intra-cavity the laser operates CW at λ_0=1563.4 nm with a linewidth of $\delta\lambda$ = 0.26 nm, as shown in Fig.2a. To show a passive mode locking operation regime we insert into CW ring cavity a sample of single wall carbon nanotube (SWCNT) fabricated by the method described in [3] that works as a saturable absorber. The laser generated a pulse train with frequency of 21.7 MHz as shown in Fig. 2c. At this regime the laser has a broader linewidth of 1.65 nm (Fig. 2b), which was obtained with pump near threshold.

l Setup

Campus São Paulo: *Rua da Consolação, 896 ● Consolação ● São Paulo - SP ● CEP 01302-907*
Tel. (11) 3236-8444/8633 ● www.mackenzie.br/mackpesquisa
mackpesquisa@mackenzie.br

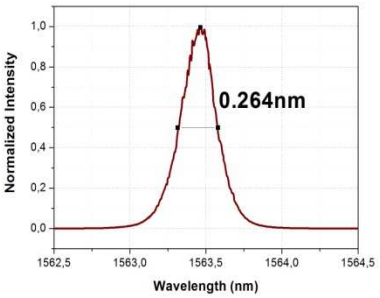

Fig. 2a) CW laser linewidth without AWGs

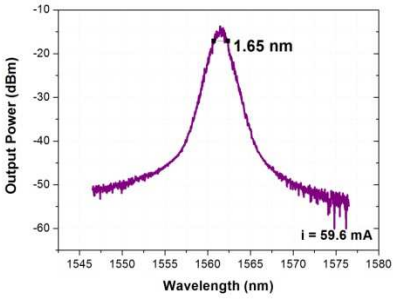

Fig. 2b) Passive mode locking laser linewidth broadened by SWCNT.

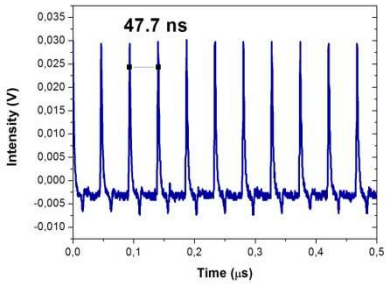

Fig. 2c) Generated pulse train by SWCNT

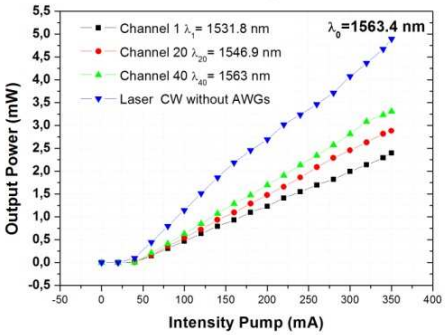

Fig 3a) Efficiency of each channel.

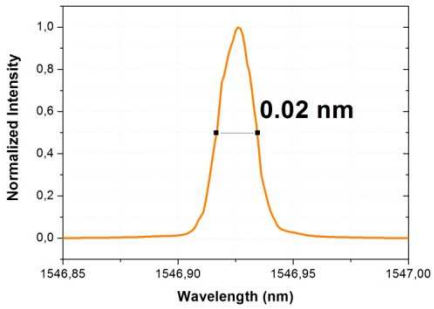

Fig. 3b) Line width at matched channel in CW regime, limited by OSA resolution

Inserting AWGs into the cavity the efficiency of few channels were measured individually and compared to the laser without AWG (Fig. 3a). The laser is more efficient for longer wavelengths. Fig.3b shows the laser linewidth, for each channel in CW operation that is limited by the optical spectrum analyzer resolution.

Fig. 4a shows the setup to insert the SWCNT between the two AGWs in the cavity to obtain the passive mode locking operation. A stable pulse train with little noise was obtained as show at Fig. 4b. Due to the increasing of intracavity losses the passive mode locking linewidth was not as broad as it could be, however it was enough to demonstrate the principle.

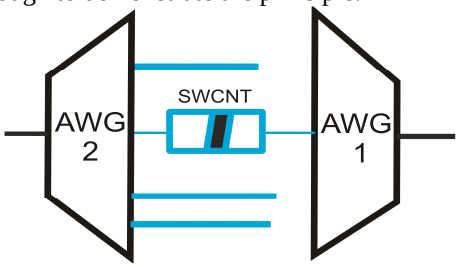

Fig. 4a) Sample of SWCNT between AWGs for passive mode lock.

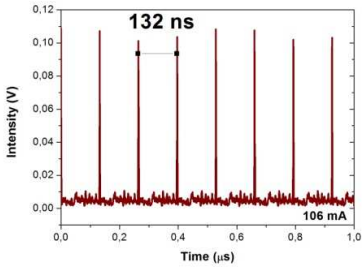

Fig. 4b) Generated pulse trains by SWCNT.

The other operating regime tested was the active mode-locked at different rates. We insert an amplitude modulator between channels number 40 due to its lower losses (Fig. 3a), and we observe pulse formation and broadening of linewidth. Fig. 5a shows that pulse duration as function of the mode-locked rates are in good aggrement with Kuizenga`s Theory [4], although we have some troubles due inhomogeneous broadening of Erbium transitions. Fig. 5b shows the respective spectrum as a function of the modulation frequency. Fig. 5c shows linewidth of channel 40 active mode-locked at 7.0 GHz with a bandwidth of 0.13 nm. And Fig. 5d shows the pulse trains generated with pulse duration about 30 ps.

To generated simultaneous multifunctions we turn on the trhee regimes togheter, channel 38 in passive mode-
locked by SWCNT, channel 39 CW and finally, channel 40 active mode-locked at 7.0 GHz. We can see the simultaneous

Campus São Paulo: *Rua da Consolação, 896 ● Consolação ● São Paulo - SP ● CEP 01302-907*
Tel. (11) 3236-8444/8633 ● www.mackenzie.br/mackpesquisa
mackpesquisa@mackenzie.br

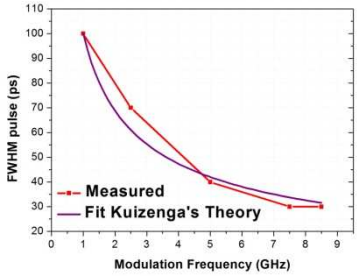

Fig. 5a) Active mode-locked rate x pulse duration

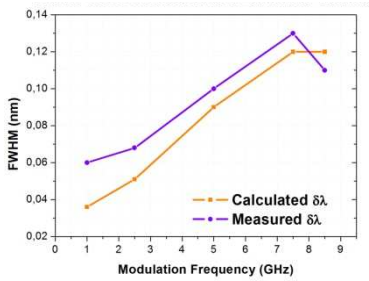

Fig. 5b) Laser linewidth as a function of the modulation frequency.

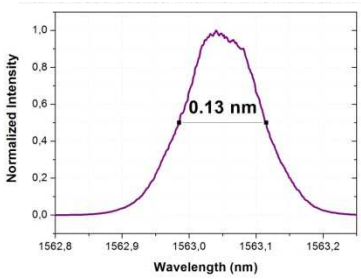

Fig. 5c) Output spectrum of an active mode-locked generated pulse trains at 7.0 GHz

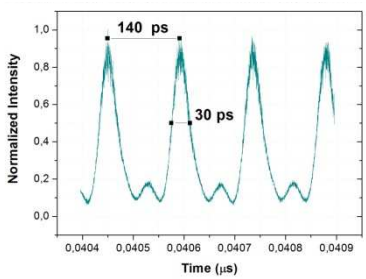

Fig. 5d) Active mode-locked channel linewidth at 7.0 Ghz

spectral at Fig. 6a. Fig. 6b shows the pulse trains and a broadening of pulse duration, probably because the linewidth spectral shape did not keep controlled and we could see many pics reflections on AML spectral channel (Fig. 6a). Fig. 6c shows a not good PML but, we can realize a modulation in a repetition time that is near to PML at channel 36 showed at Fig. 4b.

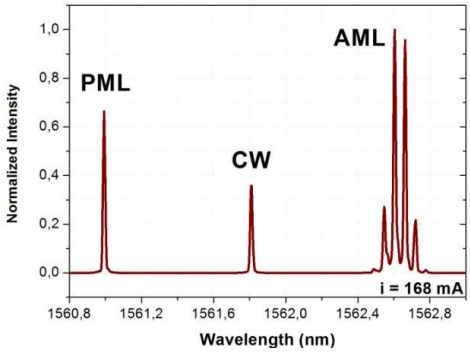

Fig. 6a) Simultaneous regimes: Passive Mode Locking (PML), Continous Wave (CW) and Active Mode Locking (AML).

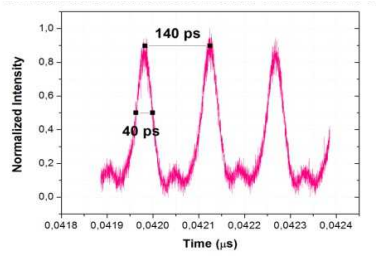

Fig. 6b) Simultaneous active mode-locked at 7.0 GHz

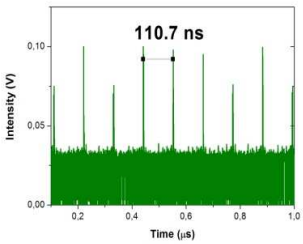

Fig. 6c) Simultaneous passive mode-locked channel by SWCNT

3. Conclusion

In conclusion, we present a multifrequency and multifunctional EDFL, good as WDM system, by integration of two AWGs into cavity, where a single gain mediun allows laser emission in 40 different channels. We demonstrate three regimes, passive mode-locked, by Single Waled Carbon Natotubes, continuous wave and active mode-locked at 7.0 GHz, simultaneously.

ACKNOWLEDGMENT

Authors would like to thank Henrique Guimarães Rosa for the SWCNT samples. This work was financial supported by Fundo Mackenzie de Pesquisa (MACKPESQUISA) and CNPq.

4. References

[1] N. Park, J.W. Dawson, and K.J. Vahala. *Multiple Wavelength Operation of an Erbium-Doped Fiber Laser*. IEEE Photon. Techn. Lett., **4**, No. 6/June, 1992, pp. 540-541.

[2] J. –N. Maran and S. LaRochelle, P. Besnard. *Erbium-doped fiber laser simultaneously mode locked on more than 24 wavelengths at room temperature*. Opt. Lett., **28**, No. 21/ November 1/2003, pp. 2082-2084.

[3] H.G. Rosa and E. A. de Souza. *Thin films incorporating carbon nanotubes used as saturable absorbers to passively mode-lock Erbium doped-fiber laser*. International Microwave and Optoelectronics Conference, Pará, 2009, pp 453-455.

[4] D.J. Kuizenga, A.E. Siegman. *FM and AM Mode-Locking of the Homogeneous Laser – Part I: Theory*. IEEE Journal of Quantum Eletronics, **QE6**, No. 11, November/1970, pp. 694-708.

2.6. Characterization of an Asynchronously Mode-locked Erbium-doped Fiber Laser Operating at 10GHz

Camila C. Dias and Eunézio A. de Souza
Laboratório de Fotônica, Universidade Presbiteriana Mackenzie, Brazil
Email: milacdias@yahoo.com.br

INTRODUCTION. The asynchronous mode-locking is been investigated as one of the techniques to obtain ultrashort pulses at high repetition rate [1, 2]. It is achieved by detuning the modulation frequency few kHz from synchronous mode-locking. In this work, we investigate the dynamic operation of an asynchronous mode-locking Erbium-doped fiber laser as a deviation from the synchronous regime [3]. In optimal operation conditions the laser produces pulses of approximately 400 fs nearly transform-limited [4].

EXPERIMENTAL METHODS. The experimental setup used to asynchronous mode-lock the laser is showed in Fig.1. It consists of an Erbium doped fiber with 1.2 m of length pumped by two diode lasers in 980 nm and 1480 nm where each WDM works as a filter to the other wavelength blocking the returning light from laser cavity to the pump. The polarization controller PC1 has the function of adjusting the state of polarization in order to optimize the power and switching within the cavity. The isolator inside the cavity allows that the propagation of light in the cavity is just in a single direction. The phase modulator with polarization maintaining fibers operates at 10 GHz. The polarization controller PC2 inserted in the cavity before the modulator optimizes the polarization state. At the laser output we used an isolator to prevent any returning signal that can disturb the laser operation. The total length of the laser cavity is approximately 18 m, which corresponds to a fundamental repetition rate of approximately 11 MHz [5].

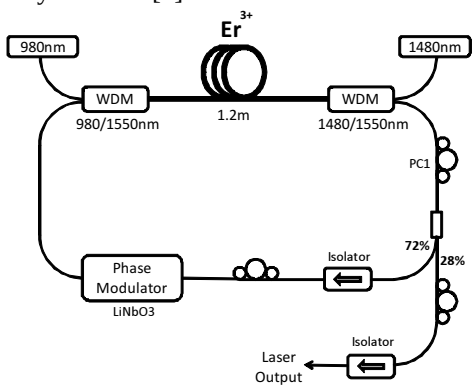

Fig. 1. Experimental setup of the Erbium doped fiber laser asynchronous mode-locked operating at 10 GHz.

RESULTS AND DISCUSSION. To understand the asynchronous mode-locking behavior we measured the optical and electrical spectra as a function of the modulation frequency detune having as reference the best point of operation of the synchronous mode-locking. The electrical spectrum was measured near DC and at 10 GHz. When the laser is synchronously mode-locked both electrical spectra are clean showing no side bands. As we detuning the modulator few kilohertz we observe peaks near DC and at the central frequency, as showed in Fig. 2 a) and b), respectively. Usually this level of perturbation is enough destroy the pulses, however in the asynchronous regime this is what is necessary to make it works better.

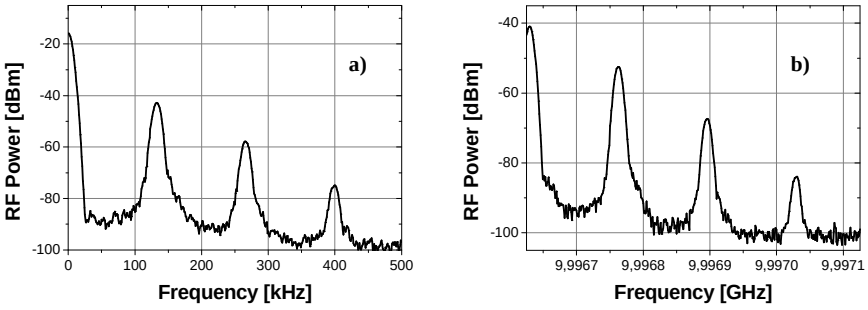

Campus São Paulo: *Rua da Consolação, 896 ● Consolação ● São Paulo - SP ● CEP 01302-907*
Tel. (11) 3236-8444/8633 ● www.mackenzie.br/mackpesquisa
mackpesquisa@mackenzie.br

Fig. 2. Electrical spectra after detuning, a) near DC frequency and b) at 10GHz.

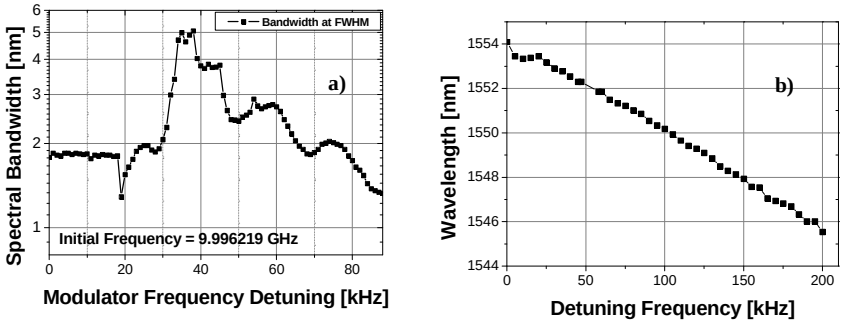

Fig. 3. a) Spectral bandwidth behavior when the laser is detuning few kilohertz from the synchronous mode-locking regime. b) Decreasing of the central wavelength as a function of the detuning, as expected.

Fig. 3.a) shows the optical spectrum behavior as a function of the detuning where we measured the variation of bandwidth at full width at half maximum (FWHM). As reference we used the best point of operation of the synchronous mode-locking. By detuning de modulation frequency tens of kilohertz we observed that instead of been destroyed the pulse bandwidth broads and becomes in some points even more stable. This broadening process reaches its maximum around 38 kHz and this point where the laser has its best performance. Since the modulation frequency is detuned few kilohertz from the cavity harmonic, in order to synchronize them the pulse has to increase its group velocity and therefore change the center frequency to maintain the mode lock stable.

Fig. 3.b) shows the decreasing of the pulse peak wavelength as a function of the detuning. As expected, in order to keep the mode lock stable the center of the pulse which has higher intensity generates more bandwidth via self-phase modulation. Therefore with more frequencies the pulse shifts its center frequency to shorter wavelength and speed up to be in phase with the modulator. The lower intensity part of the original pulse which does not have enough energy to make this shift is therefore filtered out.

Fig. 4 shows the output pulse spectra of the synchronous (dashed curve) and the asynchronous (solid curve) mode locking operation regimes where the pulse center frequency at asynchronous mode-locking is shifted to shorter wavelength. Also, the asynchronous mode-locking generates a broader spectrum with side peaks which represents a clear evidence of solitonic effects inside the cavity responsible for this mode locking mechanism.

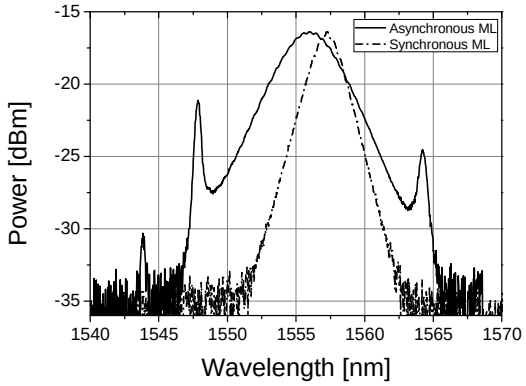

Fig. 4. Output optical spectra of the synchronous (dashed curve) and the asynchronous (solid curve) mode-locking regimes.

CONCLUSIONS. In conclusion we investigated the dynamic operation of an asynchronous mode-locking Erbium-doped fiber laser as a deviation from the synchronous regime. We observed that soliton pulse inside the cavity changes its speed decreasing the central wavelength to achieve the asynchronous mode-locking.

Acknowledgements. The authors would like to thank MackPesquisa, CNPq, and INCT-Fotonicom for financial support.

1 J. C. X. Yu, H. A. Haus, E. P. Ippen, W. S. Wong, and A. Sysoliatin, in Opt. Lett. 25, 1418, 2000.
2 W.W. Hsiang, C.Y. Lin, M.F. Tien, and Y. Lai, in Opt. Lett. 30, 2943 (2005).
3 D.J. Kuizenga, A.E. Siegman, in IEEE J. Quantum Electron. 6, 694, 1970.
4 E.S. Boncristiano, L.A.M. Saito, and E.A. de Souza, in Microw. and Opt. Techno. Lett. 50, 2994, 2008.

Campus São Paulo: *Rua da Consolação, 896 ● Consolação ● São Paulo - SP ● CEP 01302-907*
Tel. (11) 3236-8444/8633 ● www.mackenzie.br/mackpesquisa
mackpesquisa@mackenzie.br

5 C.C. Dias, E.A. de Souza, in SBMO/IEEE MTT-S International Microwave & Optoelectronics Conference (IMOC2009), 710, 2009.

2.7. Gain bandwidth optimization of an O-band Raman amplifier based on genetic algorithm

David Steinberg,[1,*] Eunézio Antônio de Souza,[1] Pedro Paulo Balbi Oliveira,[1] and Lúcia Akemi Miyazato Saito[1]

[1]*Mackenzie Presbyterian University, 930 Consolação Street, São Paulo,Brazil*
[*]*david.steinberg@osamember.org*

Abstract: In this work, a Lumped Raman Amplifier (LRA) gain bandwidth was optimized in the O-band region by using genetic algorithm. The best pump configuration was obtained for 6 km length of DCF (Dispersion Compensating Fiber) as LRA gain medium. The main objective was to optimize a 70 nm LRA gain bandwidth with ripple gain of 0.5 dB and net gain of 10 dB. With these fixed parameters, the pump number was varied until achieve the minimum ripple gain. It was verified that the pump number less than four, the ripple gain values were larger than 2 dB. However, for five, six and seven pumps the best ripple gain results were 1.51, 1.66 and 0.68 dB respectively. The smallest ripple gain result was 0.35 dB obtained for 62 WDM channels with 200 GHz spacing by using eight backward pumps which the best pump configuration was 1196.66[1], 1204.97[2], 1221.77[3], 1233.73[4], 1244.34[5], 1247.39[6], 1260.83[7], 1268.80[8] nm and 338.97[1], 93.55[2], 41.50[3], 27.85[4], 13.49[5], 6.17[6], 0.310[7] e 10.92[8] mW respectively. The LRA noise figure performance was also verified for this case.

OCIS codes: (060.0060) Fiber optics and optical communications; (060.4510) Optical communications

References

1. Namiki, S., Emory N., "Ultrabroad-Band Raman Amplifiers Pumped and Gain Equalized by Wavelength-Division-Multiplexed High-Powers Lasers Diode", IEEE Journal on Selected Topics in Quantum Eletronics **7**, 3-16 (2001).
2. H. Kidorf, K. Rottwitt, M. Nissov, M. Ma, and E. Rabarijaona, "Pump interactions in a 100-nm bandwidth Raman amplifier", IEEE Photonics Technology Letters **11**, 530-532, (1999).
3. X. M. Liu and B. Lee, "Optimal design of fiber Raman amplifier based on hybrid genetic algorithm", IEEE Photonics Technology Letters **16**, 428-430, (2004)
4. Xiau, P., Zeng, Q., Huang, J. and Liu, J., "A new optimal algorithm for multi-pump sources distributed fiber Raman amplifier", IEEE Photonics Technology Letters **15**, 206-208, (2003).
5. Yan, M., Chen, J., Jiang, W., Li, J., Chen, J. and Li, X. "Automatic design scheme for optical-fiber Raman amplifiers backward-pumped with multiple laser diode pumps", IEEE Photonics Technology Letters **13**, 948-950, (2001).
6. Jiang, H. M., Xie, K. and Wang, Y. F., "Shooting algorithm and particle swarm optimization based Raman fiber amplifiers gain spectra design", Optics Communication **283**, 3348-3352, (2010).
7. Perlin, V. E. and Winful, H. G., "Optimal Design of Flat-Gain Wide Band Fiber Raman Amplifiers", Journal of Lightwave Tech **20**, 250-254, (2002).
8. Perlin, V. E. and Winful, H. G., "On distributed Raman amplification for ultrabroad-band long-haul WDM systems," Journal of Lightwave Tech **20**, 409-416, (2002).
9. Grant, A. R., "Calculating the Raman pump distribution to achieve minimum gain ripple", IEEE Journal of Quantum Eletronics **38**, 1503-1509, (2002).

1. Introduction

The dramatic growth of the internet has invited unprecedented rapid deployment of wavelength-division-multiplexing (WDM) transmission systems based on Erbium-doped fiber amplifiers (EDFAs), which are a cutting-edge technology yet. As a result, WDM transmissions are now using up entire gain band of EDFA, i.e., C and L bands.

Because the gain bandwidth of EDFA is much narrower than the loss window of standard optical communication fibers, there is growing interest in wideband flat-gain fiber amplifiers to exploit more of the available fiber bandwidth and increase the capacity of WDM systems.

One of the most promising technologies that can help overcome the bandwidth demand is the multiple pumps Raman amplifiers being possible to achieve gain bandwidths of 10 to 12 THz (80 to 100 nm). The advantages of Raman amplifiers over EDFAs and the other optical amplifiers include the possibility of operating in any optical transmission band and superior noise performance of distributed amplification [1].

On the other hand, there are the fiber optical parametric amplifiers (FOPAs) have attracted recent attention in a number of fields due to applicability in optical amplification. Even though FOPAs may have more advantage on pump number and high bandwidth in the process of amplification, Raman amplifiers have a large technological and commercial maturity in addition to not needing a specific type of fiber for the Raman amplification generation.

For multiple pumps Raman amplifiers, the gain profile can be adjusted by appropriately choosing the relative positions and powers of the pump waves. However, the inverse Raman amplifier design problem has many difficulties such as the pump-pump, signal-signal and pump-signal interactions [2].

Several algorithms have been developed to deal with the inverse design problem, including genetic algorithm [3], neural network [4], simulated annealing [5], swarm particle optimization [6], etc. These methods have been applied on solving the inverse problem of distributed Raman amplifiers design in commercial bands (C, L and S) in WDM systems. In our paper, we optimized the gain bandwidth of an O-band lumped Raman amplifier (LRA) using genetic algorithm as our optimization method.

2. LRA optimization

2.1. Setup

We simulated the LRA optimization by using a commercial simulator called VPI. The simulation scheme is shown in figure 1:

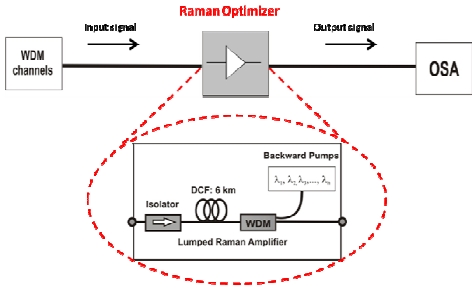

Fig. 1. Lumped Raman amplifier optimization scheme.

In real transmission links, the WDM signal channels propagate through the transmission fiber up to find the lumped Raman amplifier. In our configuration, the LRA is represented by a **Raman optimizer** block which contains the genetic algorithm responsible for pump wavelengths and pump powers optimization.

2.2. Input Parameters

In the beginning of simulation, we set the input parameters of WDM signal channels and the fiber, which are shown in table 1.

Table 1. Input parameters of WDM channel and the fiber

Input parameters	Values
Signal channels number	62
Channel spacing	200 GHz (0.8 nm)
Channel power	-60 dBm (10^{-9} W)
Transmission band	1275-1345 nm (O-band)
Fiber type	Dispersion Compensating Fiber (DCF)
Fiber length	6 km

In our configuration, 62 channels are spaced 200 GHz from 1275 to 1345 nm, each with initial power of -60 dBm. The fiber type used is a DCF (Dispersion Compensating Fiber) with length of 6 km.

Next, we set the input parameters of Raman optimizer, which are shown in table 2.

Table 2. Input parameters of Raman optimizer

Input parameters	Values
Pump number	1 to 10 pumps
Net gain	10 dB

Campus São Paulo: *Rua da Consolação, 896 ● Consolação ● São Paulo - SP ● CEP 01302-907*
Tel. (11) 3236-8444/8633 ● www.mackenzie.br/mackpesquisa
mackpesquisa@mackenzie.br

Pump wavelength optimization band	1190 – 1290 nm
Pump power optimization band	0.1 – 500 mW
Goal gain bandwidth	70 nm

Pump wavelength and pump power optimization bands are referred to genetic algorithm search space being fixed in 1190-1290 nm and 0.1-500 mW for achieving the peak Raman gain in the chosen band (1275-1345 nm). The pump number parameter was varied during the simulations.

3. Optimization Process

3.1. Optimum wavelengths and path-averaged pump powers

The calculations are fastest at consideration of pump-signal interactions and fiber attenuation, while other effects are ignored. With this approximation, the genetic algorithm finds the optimal wavelengths and path-averaged pump powers [7, 8] (over the length of the fiber) which provide the minimum deviation of **approximate gain** from the goal gain (the optimal configuration is generated for only backward pumps).

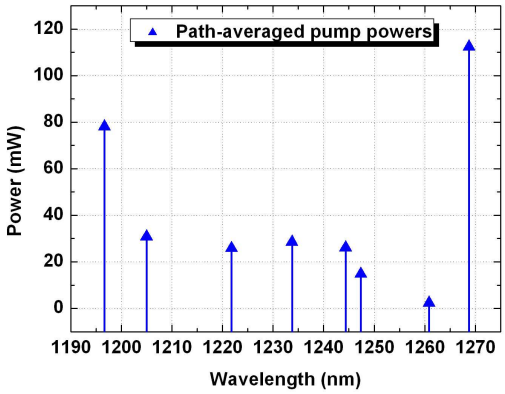

Fig. 2. Optimal backward pump configuration.

Table 3. Optimal pump wavelengths and path-averaged pump powers.

Pumps	Wavelength (nm)	Path-averaged power (mW)
1	1196.66	78.05
2	1204.97	30.84
3	1221.77	25.82
4	1233.73	28.51
5	1244.34	26.08
6	1247.39	14.77
7	1260.83	2.30
8	1268.80	112.39

Note that the last pump has a higher power than the others mainly because of DCF gain profile which means that longer wavelength signals require more power so they can achieve the same gain than shorter wavelengths.

3.2. Launched pump powers

The pump configuration found by the GA is used for the full optimization which all physical effects that were ignored, i.e., signal-signal, pump-pump Raman interactions and noise effects are now considered to calculate the launch pump powers [9].

Campus São Paulo: *Rua da Consolação, 896 ● Consolação ● São Paulo - SP ● CEP 01302-907*
Tel. (11) 3236-8444/8633 ● www.mackenzie.br/mackpesquisa
mackpesquisa@mackenzie.br

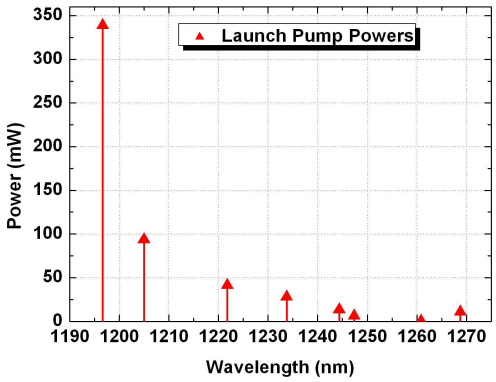

Fig. 3. Backward launch pump powers.

Table 4. Launch pump powers

Pumps	Wavelength (nm)	Launch pump power (mW)
1	1196.66	338.97
2	1204.97	93.55
3	1221.77	41.50
4	1233.73	27.85
5	1244.34	13.49
6	1247.39	6.17
7	1260.83	0.310
8	1268.80	10.92

Because of pump-pump Raman interactions, the shorter wavelengths have greater launch powers than the longer wavelengths. This is due to the energy transfer between the pumps during their propagation through the amplifier.

4. Results

For a 70 nm gain bandwidth and net gain of 10 dB, the pump number was varied to achieve ripple gain less than 0.5 dB. By varying the pump number from one to four pumps, there was no filling of the corresponding band causing a very large increase in ripple gain.

For five, six and seven pumps, it was obtained ripple gain values of **1.51**, **1.66** and **0.68** dB respectively. Note that these results were above 0.5 dB.

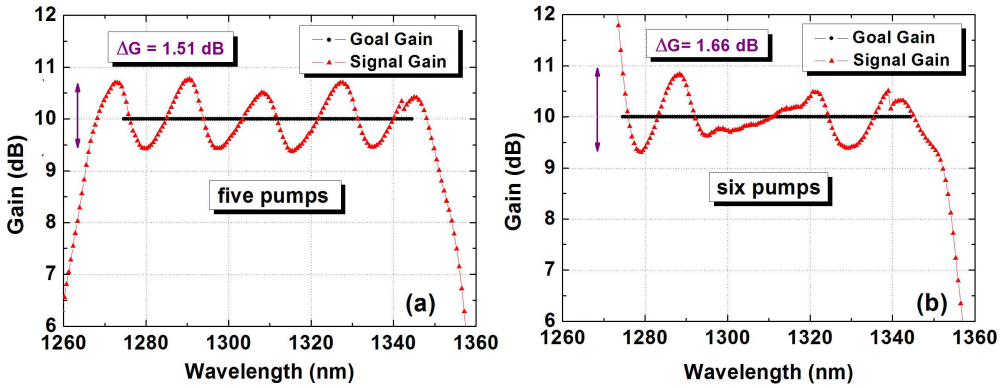

Campus São Paulo: *Rua da Consolação, 896 ● Consolação ● São Paulo - SP ● CEP 01302-907*
Tel. (11) 3236-8444/8633 ● www.mackenzie.br/mackpesquisa
mackpesquisa@mackenzie.br

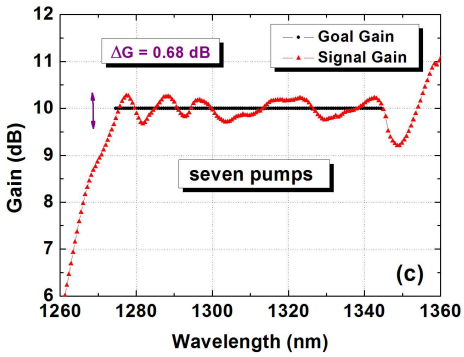

Fig. 4. Ripple gain results for (a) five, (b) six and (c) seven backward pumps.

And the best ripple gain result was obtained for eight backward propagation pumps. Its value achieved **0.35 dB**. The gain profile and the optimal pump configuration values are shown in fig. 5 and table 5 respectively.

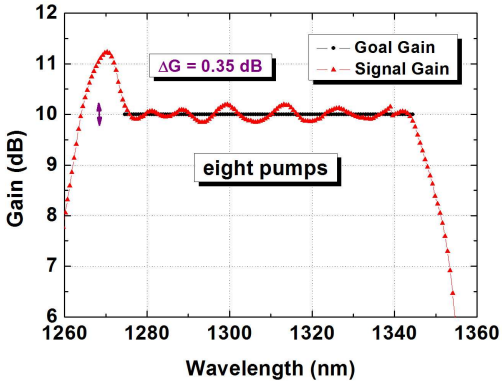

Fig. 5. Best ripple gain result of 0.35 dB for 62 WDM signal channels.

Table 5. Optimal wavelengths and powers of eight backward pumps

Pumps	Wavelength (nm)	Power (mW)
1	1196.66	338.97
2	1204.97	93.55
3	1221.77	41.50
4	1233.73	27.85
5	1244.34	13.49
6	1247.39	6.17
7	1260.83	0.310
8	1268.80	10.92

5. Noise Figure

The analysis of noise in a Raman amplifier is an essential step to understand how the signal is degraded and parameters such as the fiber length, gain, and temperature are directly related to the behavior of the noise within the amplifier. The LRA noise performance is shown in fig. 6.

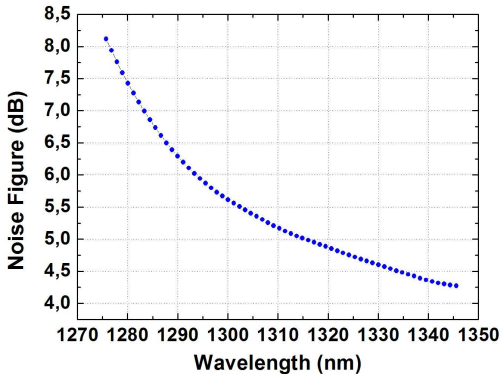

Fig. 6. LRA noise figure performance.

Campus São Paulo: *Rua da Consolação, 896 ● Consolação ● São Paulo - SP ● CEP 01302-907*
Tel. (11) 3236-8444/8633 ● www.mackenzie.br/mackpesquisa
mackpesquisa@mackenzie.br

The shorter wavelength signal show high levels of noise figure and the longer wavelengths have lower values due to the contribution of phonon-stimulated optical noise that is created when the wavelength of the signals being amplified resides spectrally close to the pump wavelengths used for amplification.

6. Conclusions

Based on genetic algorithm, we optimized an O-band LRA of 70 nm gain bandwidth obtaining the ripple gain for each pump configuration. Considering a DCF fiber as the LRA gain medium, we obtained the best ripple value of 0.35 dB with eight backward pumps for 62 WDM signal channels and we analyzed the noise figure performance for this case.

Campus São Paulo: *Rua da Consolação, 896 ● Consolação ● São Paulo - SP ● CEP 01302-907*
Tel. (11) 3236-8444/8633 ● www.mackenzie.br/mackpesquisa
mackpesquisa@mackenzie.br

3. DISCUSSÃO E CONCLUSÕES

Os resultados obtidos até o momento demonstram a potencialidade do projeto proposto e uma constante evolução e amadurecimento dos trabalhos. As partes I e II dos objetivos demonstram que a tecnologia de transmissão em altas taxas é um desafio, tanto do ponto de vista científico quanto do tecnológico. O objetivo maior do grupo é o domínio da geração e transmissão de dados em altas taxas, desenvolvendo fontes alternativas confiáveis e analisando os impedimentos inerentes a esta transmissão. Os resultados obtidos até o mementos serão aplicados aos lasers operando a 40 Gbit/s ou a taxas mais elevadas.

Data: 31/01/2011 Local: São Paulo, SP

Assinatura:

Observações:

Campus São Paulo: *Rua da Consolação, 896 ● Consolação ● São Paulo - SP ● CEP 01302-907*
Tel. (11) 3236-8444/8633 ● www.mackenzie.br/mackpesquisa
mackpesquisa@mackenzie.br